Invited Paper

Navy DAS Program for SBIRST

by
E.H. Takken[1] and J.R. Waterman[1]
Naval Research Laboratory, Washington, DC 20375
and
K.C. Hepfer[1]
Naval Surface Warfare Center, Dahlgren, VA 22448

ABSTRACT

Programs in both the U.S. and Britain[2] are attempting to apply staring array technology to the ship-board infrared search and track (SBIRST) problem. A prime objective is to speed processing time, the previous generation of 360 deg scanners having a refresh rate of only 0.5-1.0 Hz. Another objective is to enhance sensitivity using much longer integration times. An impediment, though, is that if all pixels of resolution angle ø were to be viewed simultaneously with dedicated detectors each of width w, the total net length of detector material would then have to be very large: $2\pi w/ø = 1.57$ m = 60" for 100 µRad resolution and 25 µm detectors. So the application of staring array technology to horizon surveillance needs some form of wide viewing technique involving a combination of asymmetric resolution, reduced resolution, split optics or LOS stepping. The present paper suggests that conventional NEI is not the preferred unit of measure for guiding design choices but that instead a form of BLIP S/N can be both simple and intuitive. This S/N unit of measure is used to compare the two main choices for how to adapt staring technology to the horizon surveillance problem.

Keyword List: IRST, SBIRST, missile detection, horizon search, infrared surveillance, focal plane array, staring array

1 INTRODUCTION

The camera development funded by the Office of Naval Research (ONR) is being called Distributed Aperture Sensor (DAS). Three full-staring cameras are being built using 5:1 aspect mid-wave arrays 2560 detectors long and with 2.56:1 aspect anamorphic optics. The net 12.8:1 asymmetry is needed to allocate detectors into the low horizon search region. This achieves sensitivity for dim, subsonic missile detection and emphasizes elevation resolution for discerning the dim threat just above the horizon. The cameras will be fielded and tested against aircraft and drone targets in 2005. Also being studied is a line-of-sight (LOS) stepping technique that is here called "mod-stare." The term is used to distinguish fast dedicated mirror stepping from inadequately slow gimbal step-stare.

2 THREAT SIGNATURE MODELING

2.1 Spectral Bands

Anti-ship cruise missiles are often powered by turbojets or ramjets with little plume emission. This means that the signature to be detected by SBIRST is mostly the contrast of thermal emission from warm Mach-heated dome and skin of the missile versus that from sky background. The spectral characteristics of this thermal contrast signature and its propagation through a long humid atmosphere is indicated in Figure 1. There are three spectral bands of potential interest, with the two in the mid wave called “blue” and “red.” Long-wave infrared is the band of choice for most thermal imaging applications, but for the Navy operations humid atmospheres often attenuates the long-wave signatures. Focal plane arrays are more readily available and are easier to cool in the mid-wave infrared, and the shorter wavelengths also facilitate needed resolution with small optical size.

In the mid-wave infrared the red spike band has always been the window of choice for detecting the hot CO_2 in after-burning plumes of hydrocarbon-fueled rocket motors. And the classic discrimination algorithm starting about 1960 in a

[1]Takken@nrl.navy.mil, James.Waterman@nrl.navy.mil, HepferKC@nswc.navy.mil
[2]JMDRogers@mail.dstl.gov.uk, NPTolliday@mail.dstl.gov.uk

Infrared Technology and Applications XXX, edited by Bjørn F. Andresen, Gabor F. Fulop, Proc. of SPIE Vol. 5406 (SPIE, Bellingham, WA, 2004)
0277-786X/04/$15 · doi: 10.1117/12.548360

Cincinnati Electronics single-detector dual-band scanner, has been to look for a high ratio of this bright plume CO_2 compared to potential clutter measured in the shorter blue band around 4 µm. But this use of the two mid-wave spectral bands is not applicable for the shipboard infrared surveillance problem. Shipboard IRST has to be designed to detect the more difficult low-plume turbojets with essentially just warm skin thermal emissions, and has to be able to accomplish this at long range in humid atmospheres. So for DAS, the choice is to use the high transmission blue band not as a clutter-sensing band but actually as a signal-detection band.

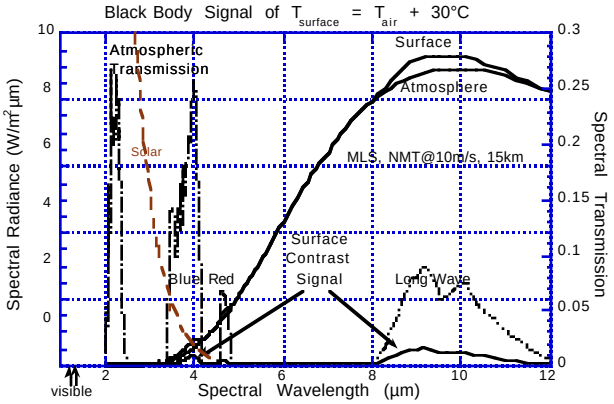

Figure 1: Black Body Absolute and Contrast Signatures After Atmospheric Transmission. There is always large, almost uniform radiation from all parts of an infrared scene, and the task of sensor design is to discern small contrast differences between pixels. There is far more thermal contrast signature emitted in the long wave infrared, but this is too often attenuated by humidity in marine atmospheres. Similarly, of the two mid-wave bands, there is more thermal contrast signature emitted in the longer wavelength red band, but this is attenuated on long paths by atmospheric CO_2. With superior atmospheric transmision, the blue band appears to offer the greatest received thermal contrast signal,. But this band is also vulnerable to degradation from solar contrast or clutter, so the DAS cameras include a filter wheel for switching between the red and blue bands depending on solar viewing conditions.

2.2 Model Thermal Signatures for Subsonic ASCM's

The stagnation temperature of air in front of a surface moving at Mach M is given by

$$T_{Mach} = T_{Atmosphere}\,(1 + .175\,M^2)\,, \tag{1}$$

where temperatures are in °K. The nose of a missile rapidly reaches this temperature, and after a short time most of the near-nose viewed surface of the missile body is close to this temperature as well. For estimation modeling the missile is treated as an effective area A of uniform temperature T_{Mach} and emissivity e. Then the contrast radiance in W/m^2Ster from this surface relative to background is

$$\partial Q = Q(T_{Mach}) - Q(T_{Bkgd},)$$

$$\approx (dQ/dT)\ (T_{Mach} - T_{Bkgd}) \tag{2}$$

$$\approx (dQ/dT)\quad .175\,M^2\,T_{Atm} \tag{3}$$

$$\approx Q\,\frac{hc/k}{\lambda T^2_{Atm}}\quad .175\ M^2\,T_{Atm} \tag{4a}$$

$$= Q\,\frac{2518\,\mu m°K}{\lambda T_{Atm}}\quad M^2 \tag{4b}$$

$$= Q\ \ 2.1\,M^2\ \ \frac{300°K}{T_{atm}}\ \ \frac{4\mu m}{\lambda}\ . \tag{4c}$$

The distinction between T_{Atm} and effective T_{Bkgd} is dropped in Equation 3. In fact, though, with good atmospheric transmission, sky backgrounds are usually quite a bit cooler than air temperature. T_{Atm} and T_{Bkgd} are closer to equal just above the horizon or in cases of strong solar forward scattering off sky aerosols, but against solar-lit clouds or water, the effective T_{Bkgd} may be higher then air temperature and ∂Q can invert to negative contrast. The step to Equation 4 assumes that the missile is subsonic rather than supersonic. Then the mid-wave spectral bands are a factor of

two or more shorter in wavelength than the peak of the thermal black-body curve, making the Boltzman equation photon quantum energy bound to $Q \propto \exp(-hc/k\lambda T)$, giving $(dQ/dT)/Q \approx hc/k\lambda T^2$ with $hc/k = 14388\ \mu m°K$.

After propagation through the atmosphere from range R, the gray-body contrast irradiance signal received at the sensor dome is

$$\partial I_{MissileOnSensorDome} = \partial Q\ eA_{Targ}\ t_{Atm} / R^2 \tag{5a}$$

and

$$\partial I_{MissileOnSensorDome} / Q(T_{Air}) = 2518\ M^2\ eA_{Targ} t_{Atm} / \lambda\ T_{Atm}\ R^2 . \tag{5b}$$

The eA/R^2 factor of Equation 5a has units of Ster, converting ∂Q radiance units of W/m^2Ster to ∂I irradiance units of W/m^2. Irradiance on sensor entrance apertures, though, is usually given in W/cm^2.

3 SENSOR MODELING

3.1 NEI and S/N

A simple expression for sensor on-dome noise-equivalent irradiance (NEI) can be derived from the definition given in Equation 6, for which all noise sources are included in $N_{Noise\ Elect}$. This is essentially the same as Equation 7 which derives electronic signal from the irradiance incident on the sensor aperture from a distant target. The irradiance units of W/cm^2 have to be multiplied first by entrance aperture area $(\pi/4)\,D^2$ to get the signal power captured by the optics, and then by integration time to get the signal energy captured per sample. The $(\pi/4)$ has been lumped into the composite parameter c along with several other constants defined in the Appendix that convert Joules at the aperture to electrons received by a (single) detector.

$$N_{Noise\ Elect/Sample} = c\ t_{int}\ D^2\ NEI , \tag{6}$$

$$N_{Sig\ Elect/Sample} = c\ t_{int}\ D^2\ \partial I_{MissileOnSensorDome} , \tag{7}$$

$$N_{Bkgd\ Elect/Sample} = x_{opt}\ c\ t_{int}\ D^2\ ø^2_{opt}\ Q_{Bkgd} , \tag{8}$$

$$N_{Noise\ Elect/Sample} = c\ t_{int}\ D^2\ ø^2_{opt}\ (dQ/dT)\ NEDT , \tag{9}$$

$$S/N = N_{Sig\ Elect/Sample} / N_{Noise\ Elect/Sample} = \partial I_{MissileOnSensorDome} / NEI \tag{10}$$

$$N_{BLIP\ Noise\ Elect/Sample} = \sqrt{N_{Bkgd\ Elect/Sample}} \tag{11}$$

The units and parameters are a little different in Equation 8 and 9, which derive electrons received from background radiance. This radiance is in units of W/m^2Ster at some unspecified range R and so to yield watts into the sensor dome has to be multiplied by both the solid angle subtense of the dome $(\pi/4)D^2/R^2$ and the emitting area $ø^2_{opt}R^2$ that a detector picks out of the distant background. The x_{opt} parameter is the reemission versus absorption ratio of the lens if its temperature is different from background and in the end will be approximated as unity. To represent the nonsymmetric aperture and resolution of the anamorphic optics of the DAS camera, D^2 and $ø^2_{opt}$ are understood to represent $D_{Az}D_{El}$ and $ø_{Azopt}ø_{ElOpt}$. Background limited performance is due to the randomness of emission of photons from the scene and conversion to electrons in the detector and is just shot noise as expressed in Equation 11. In the present discussion we distinguish between two cases of background limited performance (BLIP), sensors with either well filling or with integration time held fixed.

3.2 BLIP Well Limit for Full Staring

The simplest form of using these expressions is when t_{int} is adjusted to keep the wells filled to the level N_{well}. This is a representative approximation for a full-staring sensor. Then the value of noise electrons per sample is just $\sqrt{N_{well}}$, Equation 11 becoming Equation 12. Inverting Equation 8 gives Equation 13 for t_{int}. Equation 8 can also be written as $ct_{int}D^2 = N_{well}/(x_{opt}ø^2_{opt}Q)$ which in Equation 6 becomes the NEI expression Equation 14. Dividing Equation 5 for ∂I by this NEI gives S/N.

$$N_{\text{Noise Elect/Sample}} = \sqrt{N_{\text{well}}}\,, \tag{12}$$

$$t_{\text{int}} = \frac{N_{\text{well}}}{x_{\text{opt}}\, c\, D^2\, \text{ø}^2_{\text{opt}}\, Q_{\text{Bkgd}}}\,, \tag{13}$$

$$\text{NEI}_{\text{BLIP Well Limit}} = \frac{x_{\text{opt}}\, \text{ø}^2_{\text{opt}}\, Q_{\text{Bkgd}}}{\sqrt{N_{\text{well}}}}\,, \tag{14}$$

$$S/N_{\text{BLIP Well Limit}} = \frac{1}{x_{\text{opt}}} \frac{\partial I_{\text{Missile}}}{Q_{\text{Bkgd}}} \frac{\sqrt{N_{\text{well}}}}{\text{ø}^2_{\text{opt}}} \tag{15a}$$

$$\underset{\substack{\text{subsonic}\\ T_{\text{Bkgd}}=T_{\text{Air}}}}{\approx} \frac{2518\,\mu\text{m°K}}{l\, T_{\text{Atm}}}\; M^2\, \tau_{\text{Atm}} \frac{e\, A_{\text{Missile}}}{\text{ø}^2_{\text{opt}}\, R^2}\; \sqrt{N_{\text{well}}}\,. \tag{15b}$$

Perhaps surprising in these equations is the preeminence of resolution in the design of a full-staring sensor. S/N improves as the solid angle of optical resolution, no other sensor parameters showing, except for well filling which has a weaker dependence. And S/N improves at temperature decreases. There are, of course, tacit assumptions for this to be true.

First, the reason F-number and other efficiency parameters do not appear in NEI and S/N is that it is being assumed for the full-staring camera that integration time will be adjusted to fill the wells. The penalty is either that frame rate has to be slowed as scene temperatures decrease or else that at normal or elevated temperatures the camera is over-designed and using low duty cycle.

Figure 2 shows the integration times required to complete filling of very large wells when background temperatures change. One would expect the blue band to be somewhat photon starved in cold backgrounds, and the numerical result is that for about 10 % of weather cases it is not possible in this band to maintain both a 30 Hz frame rate and to fill large wells. On the other hand, the red band could support frame rates faster than some 120 Hz in about 10 % of warm weather cases. The dependence of S/N on well filling is rather weak in Equation 15, so the preferred method of operations may be to maintain frame rate to support declaration processing speed. It is not yet known how often the scene or crossing threats contain high frequency information to be processed. Scintillation time constants, for instance, become long when wind is down the viewing path, and threats tend to be inbound rather than crossing, so 10 Hz might be adequate for supporting declaration processing. The DAS FNC program will evaluate field data in 2005 to determine what scene refresh rates are required.

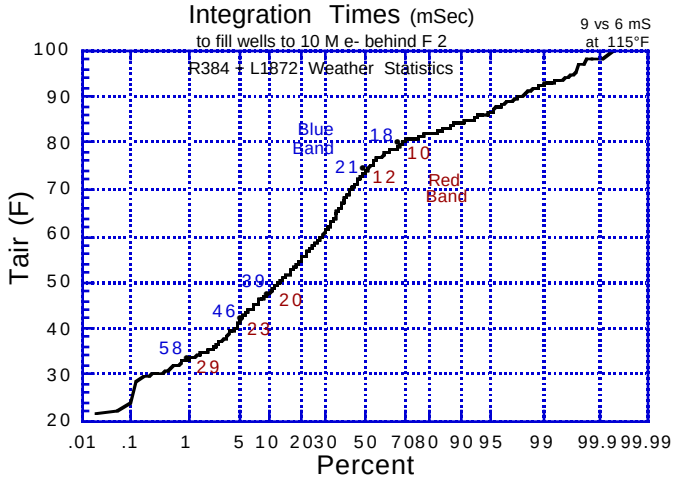

Figure 2: Well-Filling Integration Times and the Probability of Occurrence of Air Temperatures in the R384 Random Weather Data Base

3.3 Elevation Search Coverage

The eA/ϕ^2R^2 term in Equation 15 is the ratio of the missile effective area to the projected optical resolution footprint at range. This $1/\phi^2$ dependence can be written to display other optical parameters using $\phi = w_{det}/f$ and $F = f/D$ with $\phi_{opt} = \phi N_{\phi/Det}$ as, for instance,

$$S/N_{BLIP\ Well\ Limit} = \frac{\partial I_{Missile}}{Q_{Bkgd}} \sqrt{N_{well}} \frac{f_x f_y}{N^2_{\phi/Det} w^2_{det}} , \tag{16a}$$

but it is suggested that this can be subtly misleading when making judgments about sensor design. That's because the fields of view Ω_{Az} and especially Ω_{El} are systems level specification parameters and should be held fixed. It is better to use $\phi = \Omega/N_{det}$, in which case the recasting of Equation 15 is

$$S/N_{BLIP\ Well\ Limit} = \frac{\partial I_{Missile}}{Q_{Bkgd}} \sqrt{N_{well}} \frac{N_{AzDet} N_{ElDet}}{\Omega_{AzOpt} \Omega_{ElOpt}} \tag{16b}$$

This last equation makes clear[1] that a large number of detectors need to be pointed into the required search region and that detectors pointed above the search region do not contribute to improving sensitivity.

3.4 Electronic and Non-Uniformity Noise

The BLIP well limit assumption of Equation 12 is that all noise sources are less than the background shot noise of $\sqrt{N_{well}}$ electrons. In the array being purchased from Raytheon Vision Systems, the electronic noise referred back to the input is predicted to be less than 500 electrons. With that, well filling could be as low as half a million carriers and still leave background shot noise dominant. The arrays have not been delivered or even packaged yet at the time of this writing, but it is anticipated that electronic noise should not be significant even for mSec integration times.

Non-uniformity noise is the difference of response of detectors across the array to the spatially uniform component of the thermal background. It can be expressed as the fraction f of well filling N_{well}, the effective noise being $f N_{well}$. After correction the residual nonuniformity noise needs to be less than the BLIP noise, $\sqrt{N_{well}}$, so the NUC performance requirement is

$$f_{NUC\ Required} < N_{well} / \sqrt{N_{well}} = 1/\sqrt{N_{well}} \tag{17}$$

Conceptually this is the same as the noise limited contrast that the sensor is capable of detecting.

There are two factors that make NUC more difficult for full-staring SBIRST than for most mid-IR sensors. First, the emphasis on staring means long integration time with large N_{well} and hence a need for lower than normal residual nonuniformity as in Equation 17. But then also, there is the fact that one-point scene motion NUC can not be used for continual update of offset coefficients. Resolution is so important for sensitivity in Equations 14 and 15 that the sensor has to be well stabilized, and this removes scene motion. However, a long-time average of the SBIRST horizon scene should be nearly uniform azimuthally over a few degrees, and it is anticipated that this can probably be used as a calibration reference for one-point NUC. This form of one-point NUC would remove the slow elevation gradient present in most horizon scenes, but this might be good both for image display and for missile-detection processing. Numerically this is perhaps the greatest challenge and uncertainty for full success of the DAS FNC program.

3.5 BLIP t_{int} Limit

If t_{int} is held fixed rather than N_{well}, Equations 14 and 15 become

$$NEI_{BLIP\ t_{int}\ Limit} = \frac{\phi_{opt}}{D} \sqrt{\frac{x_{opt} Q_{Bkgd}}{c\, t_{int}}} \tag{18a}$$

$$= \frac{F \phi^2_{opt}}{N_{\phi/det} w_{det}} \sqrt{\frac{x_{opt} Q_{Bkgd}}{c\, t_{int}}} \tag{18b}$$

$$S/N_{BLIP\ t_{int}\ Limit} = \frac{D}{\phi_{opt}} \sqrt{\frac{c\, t_{int}}{x_{opt}}} \frac{\partial I_{Missile}}{\sqrt{Q_{Bkgd}}} \tag{19a}$$

$$= \frac{N_{\phi/det} w_{det}}{F \phi^2_{opt}} \sqrt{\frac{c\, t_{int}}{x_{opt}}} \frac{\partial I_{Missile}}{\sqrt{Q_{Bkgd}}} \tag{19b}$$

Equations 18 and 19 are the same as Equations 14 and 15 except for the change in independent variable between t_{int} and N_{well} using Equation 8 in the form $N_{well} = x_{opt} c t_{int} Q (D^2 ø^2_{opt}) = x_{opt} c t_{int} Q (N^2_{ø/det} w^2_{det}/F^2)$. The strong dependence on solid angle resolution is the same, but with t_{int} held fixed, S/N now decreases with decreasing temperature.

4 RESOLUTION AND THE HORIZON SCENE

4.1 The Need for Resolution, Stabilization and Limited Elevation Coverage

There are two reasons why very good resolution is needed. First, as has been pointed out, is the fact that resolution is so preeminently necessary in Equation 14-15 and 18-19 for achieving sensitivity.

The other reason why very good resolution is needed is that, compared to radars and even to the infrared missile warning application on aircraft, the SBIRST has only one design parameter for helping its processor distinguish missile threats from clutter—resolution. SBIRST can and must use resolution very well. Figure 3 depicts elevation angles of a possible future very low sea skimming missile as viewed from a vantage point 20 m above the water. The elevation angles are very small.

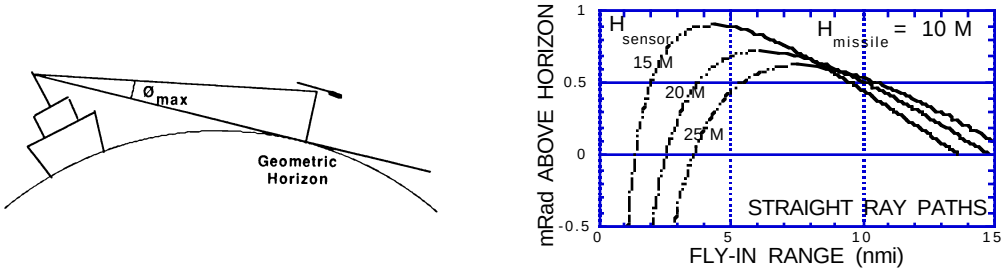

Figure 3: Approximate Elevation View Angles Of Distant Sea-Skimming Missiles

Sensor mounting needs to be high to see supersonic threats at long range. But against slow dim threats mounting needs to be low so as to minimize the chance of needing to see them against the water when they are being initially detected. So another task of the DAS program is to perform sufficient modeling, including ray bending, to determine whether a single mounting height can be optimized for both subsonic and supersonic threats.

Figure 3 is an approximation assuming straight ray paths, but in reality rays tend to bend either up or down due to air density and index gradients characterized by air versus water temperature. The statistical plot of Figure 4 indicates that air-sea temperature differences usually fall within the range of -6 to +4 °C, and Figure 5 gives a summary of the resulting ray bending along long viewing paths. Cold air bends rays upward which shortens first detection range, depresses the water line and introduces mirage. Warm air bends rays downward extending first detection range and raising the apparent elevation of sea skimmers, but usually by not more than 3 mRad ≈ 1/5 deg.

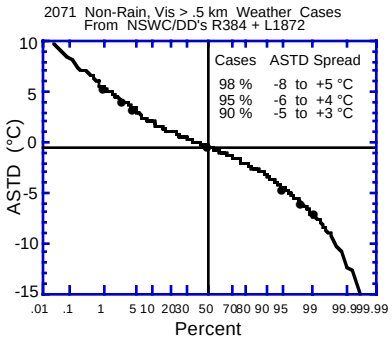

Figure 4: Frequency of Occurrence of Air vs Sea Temperature Difference

Figure 5 indicates the apparent elevation position of sea skimming missiles as a function of its range, actual height and the atmospheric air-sea temperature difference (ASTD). "Geometric horizon" is defined as that for a straight line from the sensor to a tangent skimming the curved ocean surface. "Detection horizon" is defined as the sensor viewing elevation angle at which there is a first chance for ray path connection to the inbound sea skimmer. With cold air, down bending and mirage the water-line position is depressed. The geometric and detection horizons still remain essentially equal, but the water line is below at 350-400 μRad for ASTD = -5°C. At ASTD ≈ 0.5°C gravitationally and thermally induced index gradients essentially cancel and ray paths are close to straight. Warm air makes sea skimmers appear to be higher than they would be with straight ray paths.

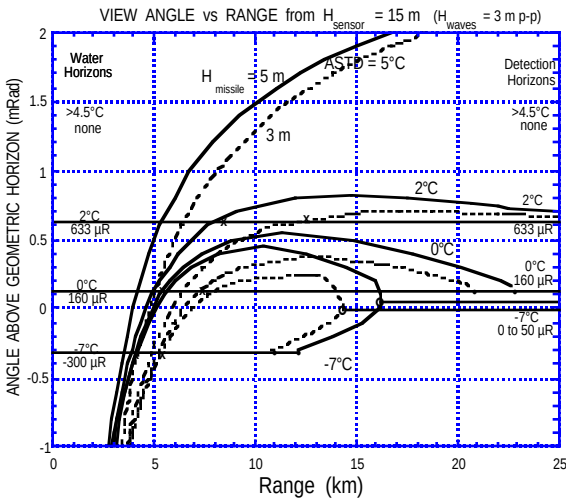

Figure 5: Detection and Water Horizons

Figure 6 shows worst-case clutter data viewed from a light house 12 mi out at sea from Cape Hatteras at a time when gulf stream boundary eddies surrounded the tower causing very cold air relative to water, ASTD = -7 to -10 °C, and hence strong ray upbending. Clouds do not usually appear below 2° but in this case are bright and structured down to below one degree. The presence of mirage is not apparent in ocean horizon scenes because the empty sky has no structure to mirage, but if a bright low-altitude missile came into view, it would appear first not at the suppressed water line but up at an elevation angle about half a milliradian higher and then split in two during ingress with one point moving upward and the mirage point moving downward until it hit the water line and disappeared. This is worst-case clutter, first because the spectral filter used to take this data was non optimal passing, shorter wavelengths of bright solar, but also because the water-horizon range is moved in so close that wave shapes are discernible and moving on the water line. Solar glints are occasionally single-pixel and sometimes even located below a dark, cloud-shaded wave crest. This ASTD is atypical, but metrology equipment is needed aboard ship to monitor when this occurrence might be happening. With more neutral air-sea-temperature-difference, wave shape is not discernible on the water horizon. When its blue spectral band is in use, the DAS cameras should see far less solar clutter than in Figure 6, and use of the red filter should remove essentially all solar radiation from the scene except in a narrow swath at times close to sunset and sunrise.

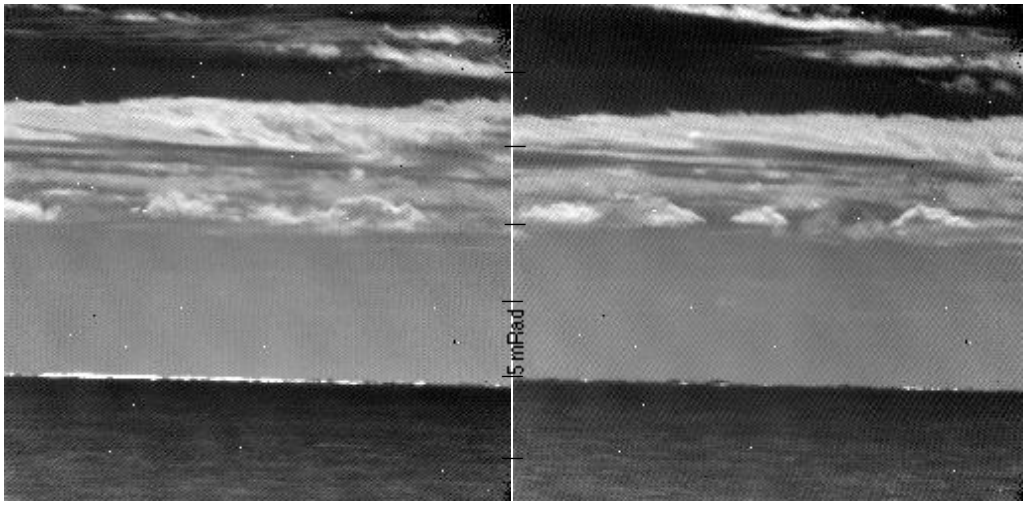

Figure 6: Horizon solar glint with shadowed foreground. ASTD = -7 to -10 °C. Mirage band ≈ 450 µRad. Sensor resolution = 125 µRad. Solar position = 30° elevation. Spectral bandpass = 3.1-4.9 µm. Radiances from low sky to glint to shadowed water are 0.20, 0.27 and 0.16 W/m^{2}Ster at the sensor. Atmospheric transmission ≈ 0.4. Time between scenes = 2 min.

A more normal but still not entirely common infrared horizon scene is reproduced in Figure 7. The elevation gradient in background radiance at the horizon is 5%/mRad, and a one pixel displacement in this gradient is large compared to a dim missile signature. Strong thermal radiance gradients can not occur without good atmospheric transmission, and fortunately, this also means that the dim threat is more likely to be first detected at longer range before it becomes viewed against the water.

The point of Figures 2-7 is that sensor elevation resolution is needed to resolve the height separation of sea skimming missiles and minimize upward blurring of ocean mean and clutter radiance. The critical search region for sea skimmers is ≈ 0.2° high by 360° around the horizon, an extremely unusual aspect ratio. For optimum sensitivity against sea skimmers the design objective is to place as many detectors as possible into this spaghetti-noodle search region. It is not possible both to do that and also accomplish surface search, and certainly not to see a high diver up at 80° elevation. The DAS camera is designed primarily for sea skimming missile detection with surface search a secondary application.

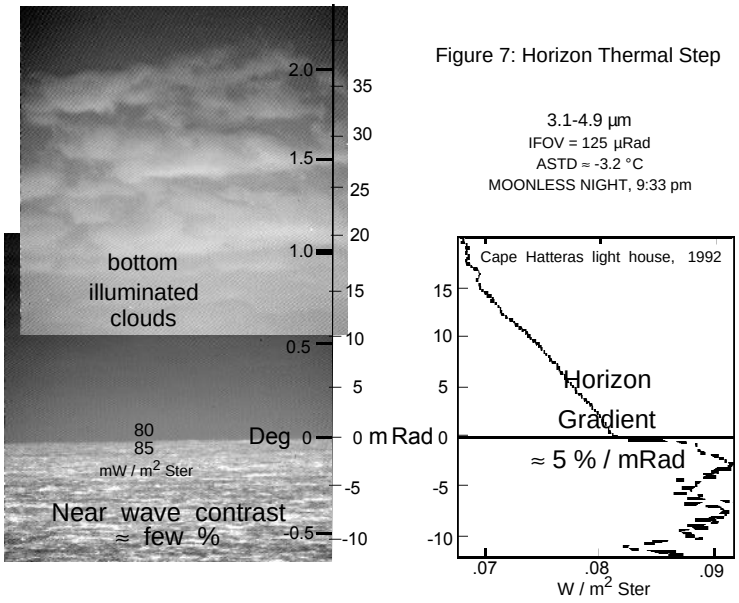

Figure 7: Horizon Thermal Step

5 SIZING DETECTORS AND OPTICS FOR DAS

The distinction between optical resolution $ø_{opt}$ and detector resolution $ø_{det} = w_{det}/f$ is important in Equations 14-15 for sensitivity. Tight optical blur is needed to match small detector size. But good F-number and wide azimuthal field of view (FOV) are needed as well, and these are conflicting design goals for optical design. The bound on these three parameters for a large sample set of high-quality lenses was found empirically to be[1]

$$ø_{opt} > 2\ \mu\text{Rad} * (\text{FOV in deg})^{1.5} / (\text{F} - 0.5)\,. \tag{20}$$

This formula was used in the specifications when soliciting proposals for DAS camera optics, and the unit now being assembled by Telic Optical is both very close to this empirical design limit and very close to diffraction limited.

The choice of detector size has to be closely linked to optical performance, and a 25 µm size was chosen for the DAS camera. 20 µm detector size would have been 20 % smaller in linear dimension offering a full 50 % reduction in dewar volume, and also of the optics if focal length and aperture were reduced in proportion. But that would have involved compromise in sensitivity. Detector resolution $ø_{det} = w_{det}/f$ would be the same with this smaller sizing, but because of diffraction limiting, optical blur $ø_{opt} > 2.44\lambda/D$, would increase by about 20 %—meaning a 35 % decrease in sensitivity according to Equations 14-15. So the detector size used is 25 µm.

Figure 8 gives a drawing of the Telic optics with RVS dewar and cryocooler compressor attached. Optics to dewar assembly is scheduled for the end of April, 2004 at NRL. NRL is also developing the processor which links to the camera via G-link fiber.

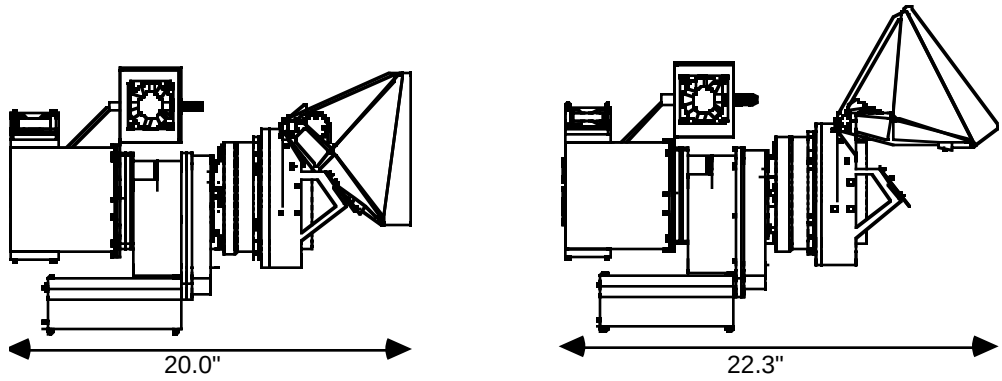

Figure 8: DAS Full-Staring Surveillance Camera. Prisms are used to achieve an anamorphic factor of 2.56. The narrow elevation FOV is intended for high-sensitivity near-horizon missile detection. With the anamorphic prisms tilted upward and out of the optical path, elevation FOV is expanded for ocean surface surveillance.

6 HORIZON SPREAD TECHNIQUES AND MOD-STARE VS FULL-STARE

Staring focal plane arrays are typically square or nearly square in shape, which normally means that many of the detectors will be directed high above the horizon. Custom long-aspect arrays, spit optics, anamorphic optics and LOS stepping are all wide-view approaches for increasing the number of detectors in the low elevation search region and thereby improving resolution and sensitivity for missile detection. The first three techniques can be used in full-staring applications. The latter when accomplished with a fast dedicated mirror is here being called "mod-stare." Another technique often discussed is "super-resolution" obtained by dither or motion of the LOS by half-pixel or smaller spacing. But this is really an anti-aliasing technique that does not fundamentally improve resolution or sensitivity. That effect is being implemented electronically in the DAS camera processor by using multiple spatially-phased matched filters.

The British program is using split optics and conventionally shaped arrays in which the improvement in sensitivity by optical relocation of detectors is a factor of two. The DAS design is combining both aspect arrays and anamorphic optics. A way to express the DAS design objective is to scale from a square array to one with the same number of detectors but azimuthal length aspect, x=5 and also effectively further squeezed down by optics with anamorphic ratio a=2.56. Compared to the square array with symmetric optics looking into the same azimuthal coverage, this brings down elevation coverage and elevation resolution by a factor of xa = 12.8 with sensitivity improved by the same factor:

$$\text{Ø}_{\text{ElOpt}} \text{ -> } \text{Ø}_{\text{ElOpt}} / (\text{xa}), \qquad \text{aspect array + anamorphic optics} \qquad (21a)$$

$$\text{S/N -> xa * (S/N) = 12.8 (S/N)}, \qquad \text{aspect array + anamorphic optics.} \qquad (21b)$$

And now this is compared to mod-stare LOS stepping, which also "pulls" detectors down into the low elevation search region by increasing focal length. This time the optical resolution shrinkage is the same in azimuth and elevation, so there must also be an accompanying compromise in integration time and well filling. If a given azimuthal coverage Ω_{AzOpt} is maintained by executing n LOS positions, resolution is improved to advantage by

$$\text{Ø}_{\text{opt}} \text{ -> } \text{Ø}_{\text{opt}} / \text{n}, \qquad \text{LOS stepping.} \qquad (22a)$$

But the disadvantage is that if refresh rate is to be maintained, integration time and well filling have to be reduced by a factor of $\text{n}/\text{e}_{\text{step}}$, were $\text{e}_{\text{step}} \approx< 0.5$ is the efficiency of the LOS stepping mechanism, e_{step} = (total time LOS stationary in cycle)/(LOS cycle time).

$$\text{N}_{\text{well}} \text{ -> } \text{N}_{\text{well}} / (\text{n}/\text{e}_{\text{step}}), \qquad \text{LOS stepping.} \qquad (22b)$$

The net effect of these two terms, Equations 22a and 22b, on Equation 15 is then

$$\text{S/N -> } (\text{n}^{1.5} / \sqrt{\text{e}_{\text{step}}}) \text{ (S/N)}, \qquad \text{LOS stepping.} \qquad (22c)$$

So to make mod-stare achieve the same azimuthal spreading sensitivity gain as that of DAS, it must be designed to have

$$\text{n}^{1.5} = \text{xa}\sqrt{\text{e}_{\text{step}}} \approx 18, \qquad \text{or} \qquad \text{n} \approx 7 \qquad (23)$$

In a hybrid mod-stare the number of steps could be reduced by using both array aspect and LOS stepping. Fewer larger steps is desirable because the time to slue an angular distance increases only as the square root of the distance.

This suggests that sensitivity should be achievable with a reasonable number of LOS step positions and probably a reasonable mechanical step-stare mirror torquer assembly. And An initial "mod-stare" design has been investigated but is not being pursued beyond tentative feasibility until it is known whether the slower 10 Hz refresh rate is suitable for fast declaration processing. A low-cost, light 5.5 oz, 7.25"x3.15" honeycomb mirror has been fabricated with transfer surface flat to λ/4, but its mechanical robustness, step cycle speed and motion breaking have not been tested. Compatible optics must have entrance pupil displaced 5-6" onto the mirror. A good ray-trace design of this has been completed, so the optics is achievable. The main advantages of mod-stare would be reduced number of focal plane arrays and therefore lower cost and weight, and reduced heat loading from cryogenics. One-point NUC could also be accomplished during the retrace. Processing would be essentially the same as for full-staring. The main disadvantages are the mechanical assembly and slower refresh rate.

7 SUMMARY

ONR is funding the development of DAS staring infrared surveillance cameras for shipboard use. For missile detection the design uses both a wide-aspect array and anamorphic optics to achieve an effective aspect ratio of 12.8 for placing a large density of detectors in a low elevation band on the horizon. For surface surveillance the design includes a flip mechanism for removing the 2.56 anamorphic element and expanding the elevation coverage. Issues to be settled include what ≥ 10 Hz frame rate is needed for fast ≈ 1 sec declaration processing, achievability of low residual nonuniformity with large wells and use of scene-based one-point NUC in the stabilized ocean-horizon scene. The system with automatic processor will be field tested against inbound aircraft in 2005.

APPENDIX: DAS FULL-STARING CAMERA PARAMETER VALUES

$c = \frac{\pi}{4} e_{cs} e_{det} e_{opt} / hn$

e_{opt} = 0.82, 0.77 for Blue vs Red bands times $e_{lowRCSwindow} \approx 0.9$

$e_{cs} \approx 1$, with cooled filter at exit pupil 80 mm above focal plane

$e_{det} \approx .8$, with ≈100 % fill factor from dry etch V-notch reticulation*

$h\nu = 7.95, 9.34 \times 10^{-19}$ J/Phot for Blue & versus Red bands

$x_{opt} = 1-(1-1/e_{opt})(Q_{opt}/Q_{Bkgd}) \approx 1$ if $T_{opt} = T_{lens}$

$N_{ø/det}$ = optical blur size / detector pitch ≈ 1.15 - 1.2

$N_{effø/det} = x_{opt} * N_{ø/Det}$

$w_{det} = 25$ μm,

F = 2

a = 2.56, optical anamorphic ratio

x = 5, focal plane array aspect ratio

Q_{Bkgd} = radiance of background in W/m^2Ster,

∂I = missile contrast signal radiance on sensor dome in W/cm^2,

*Minimal crosstalk achieved by MBE deposition of band gap gradient in detector.

ACKNOWLEDGMENTS

This work is funded by the Office of Naval Research, Surveillance, Communications and Electronic Combat Division, Code 313, Keith Krapels <KrapelK@onr.navy.mil>

REFERENCES

[1]A.F. Milton circa 1973